ENGINEERING TRANSACTIONS • *Engng. Trans.* • **60**, 1, 3–14, 2012
Polish Academy of Sciences • Institute of Fundamental Technological Research (IPPT PAN)
National Engineering School of Metz (ENIM)
SIXTY YEARS OF THE ENGINEERING TRANSACTIONS

Development of a Soft Recovery System of Supersonic Projectiles

Dong-Teak CHUNG[1)], Ihnseok RHEE[1)], Byung Yun JOO[1)], Doo Han JIN[1)],
One Kwon RIM[2)], Kwan Jin PARK[2)]

[1)] *The Korea University of Technology and Education*
School of Mechatronics and Mechanical Engineering
Cheonan, Chungnam, 330-708, the Republic of Korea
e-mail: dtchung@kut.ac.kr

[2)] *4-3, Agency for Defense Development*
Daejon, Chungnam, the Republic of Korea

An effective and robust soft recovery system for supersonic projectiles is required for the test of intelligent projectiles in development phase. The survivability of the projectiles after initial impact onto the target is the most important requirement of them. A soft recovery system, consisting of multiple equally spaced metal plates, was designed and fabricated. Numerical simulations were performed to estimate the deceleration of the projectile after piercing through a thin steel plate with various speeds. Next, the thickness distribution of the plate for uniform deceleration could be designed. An aluminum foil sensor system was used to measure the arrival time of the projectile onto each plate and multi-channel time recording system for this test was developed. Field tests were done using a rifled barrel gun and a smooth bore gun. Deceleration data were acquired successfully. The trajectories of the projectile after the impact tended to veer off from the initial firing line with an increasing yaw angle. Deceleration increased with the increase of the yaw angle. Field data were used to design a final recovery system to retrieve the projectile with a minimum deceleration and damage.

Key words: soft recovery, projectile, impact, simulation.

1. Introduction

In the field of modern weapon systems, a demand for smart and intelligent warheads with maximum effectiveness and minimum collateral damage is ever increasing. The survivability of the warheads after initial impact onto the target is the most crucial requirement of them. Traditional powder gun is the most common launching method but an initial acceleration may be too severe and may not guarantee the survival of the electronic components in the projectile.

Rocket launching method is available for a less severe initial acceleration but it requires vast resources and is time consuming. And the recovery of the projectile after initial impact with minimum damage is of the utmost importance to determine the survivability of the projectile. The technique for soft recovery of supersonic projectile is not well established yet. A few researches were published related to this subject [1]. For sub-sonic projectiles, various soft and light- weight materials are utilized to "catch" them, but in case of super-sonic projectiles the magnitude of initial deceleration is either too light or too severe and most often it ends with fractured projectiles. In this study, the numerical simulations were performed to estimate individual deceleration of the projectile after perforating the thin steel plates with various speeds. The analytical interpolation equations for the deceleration rate of projectile piercing through plates of different thickness were tabulated from the data. The optimum thickness distributions of the plates for overall uniform deceleration could be determined by utilizing the equations. And a soft recovery system, consisting of steel frame with multiple equally spaced metal plates, was designed and fabricated. Finally, the field tests were conducted using a 40 mm caliber rifled barrel gun and a 155 mm caliber smooth bore gun. The test results of 40 mm gun showed all the projectiles veered off from the initial firing line and exited at the midsection of the frame; the retrieved projectiles were damaged. The 155 mm gun test results were more satisfactory, i.e., a smooth deceleration span was much longer and the projectiles were recovered intact. Comparing the results from the two different guns we can conclude that the initial spin of the projectile attributes to faster yaw increase. Even with a perfect test condition the axis symmetric assumption cannot be maintained throughout the test. Hence, further numerical studies of three- dimensional oblique impact behavior of the projectile are required. More tests with different thickness distribution of the plates and careful alignment are needed to complete the soft recovery test.

2. Numerical simulation

At the design stage of the soft recovery system, the thickness distribution of 60 equally spaced metal plates for overall uniform deceleration of projectile was estimated by the axis-symmetric normal impact simulations, changing the striking velocity of a projectile to 200, 300, 400, 500, 600 m/s and the thickness of the plate to 0.6, 1.2, 2.3, 3.2 mm, respectively. For the simulation task, the two- dimensional Lagrangian explicit finite element program using quadrilateral element NET2D developed by Chung [2, 3] was used. The AISI 4340 steel projectile was assumed to be elastic. Dynamic behavior of the steel plate was assumed to be the Johnson-Cook model [4] as in Eq. (2.1) with material parameters as shown in Table 1. This model is the most widely used phenomeno-

Table 1. Johnson-Cook model parameters for a mild steel plate.

A [GPa]	B [GPa]	C [GPa]	n	m	T_{room} [°C]	T_{melt} [°C]
0.5320	0.2295	0.0274	0.3024	1.0	25	1520

logical ductile fracture model, which decomposes the total strain rate into an elastic and plastic portion, and involves five constants: A, B, C, n and m. It was also assumed that almost deformated energy is converted into a heat. In order to describe the ductile fracture and piercing of the plate material, the element erosion algorithm was used: when the equivalent plastic strain of an element exceeds 200%, the element is deleted and is excluded from further computation.

$$\sigma_y = (A + B\overline{\varepsilon_p}^n)\left(1 + C\log\left(\dot{\overline{\varepsilon_p}} / \dot{\overline{\varepsilon_0}}\right)\right)\left(1 - \frac{T - T_{\text{room}}}{T_{\text{melt}} - T_{\text{room}}}\right)^m. \tag{2.1}$$

It was found that the velocity reduction factor (α) of a projectile, after piercing plate, depends on both the plate thickness and the striking velocity of a projectile as shown in Fig. 1; a thicker plate with slower striking velocity produced a high reduction factor. With the simulation results, the factor α was interpolated as Eq. (2.2).

$$\alpha(t_{\text{sheet}}, V_{\text{strinking}}) = a(t_{\text{sheet}}) \exp^{-V_{\text{striking}}/\tau(t_{\text{sheet}})} + b(t_{\text{sheet}}), \tag{2.2}$$

where parametric values of a, τ, and b are summarized in Table 2.

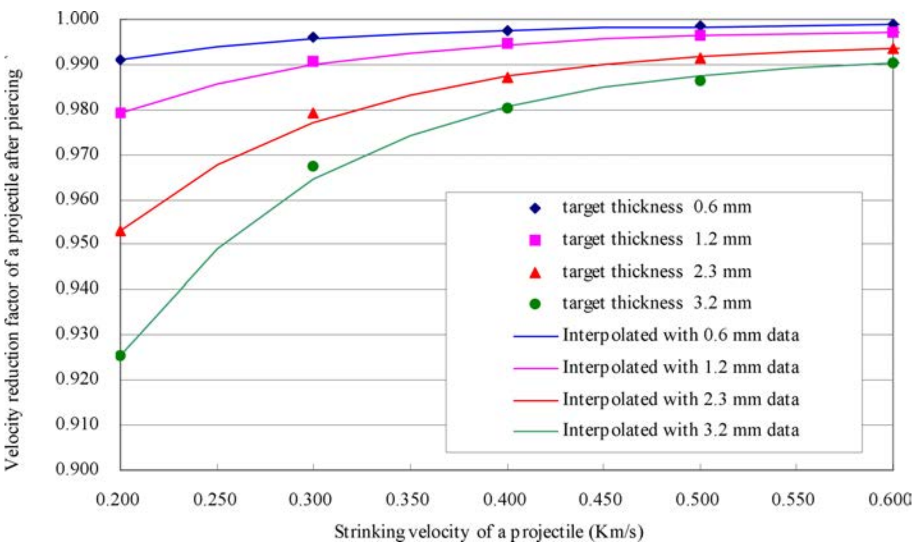

FIG. 1. Velocity reduction factors of projectile after piercing the metal plate.

Table 2. Interpolation parameters of Eq. (2.2) with various plate thicknesses.

Steel plate	Thickness: 0.6 mm	Thickness: 1.2 mm	Thickness: 2.3 mm	Thickness: 3.2 mm
a	−0.42380	−0.10103	−0.23423	−0.38021
τ	0.120482	0.117647	0.116279	0.114943
b	0.999053	0.997771	0.994868	0.992354

$$A_{\text{decel}} = \left| \frac{V_{\text{after piercing}}^2 - V_{\text{strinking}}^2}{2t_{\text{sheet}}} \right| = \left| \frac{\alpha^2 - 1}{2t_{\text{sheet}}} \right| V_{\text{strinking}}^2. \tag{2.3}$$

From Eq. (2.2) and (2.3) the average deceleration of a projectile after piercing individual plate could be estimated, and the thickness distribution of the plate for overall uniform deceleration could be designed. Figures 2a and 2b show the distribution of 60 plate arrays and the estimated deceleration of a projectile with the range of constant deceleration of about 100 000 G.

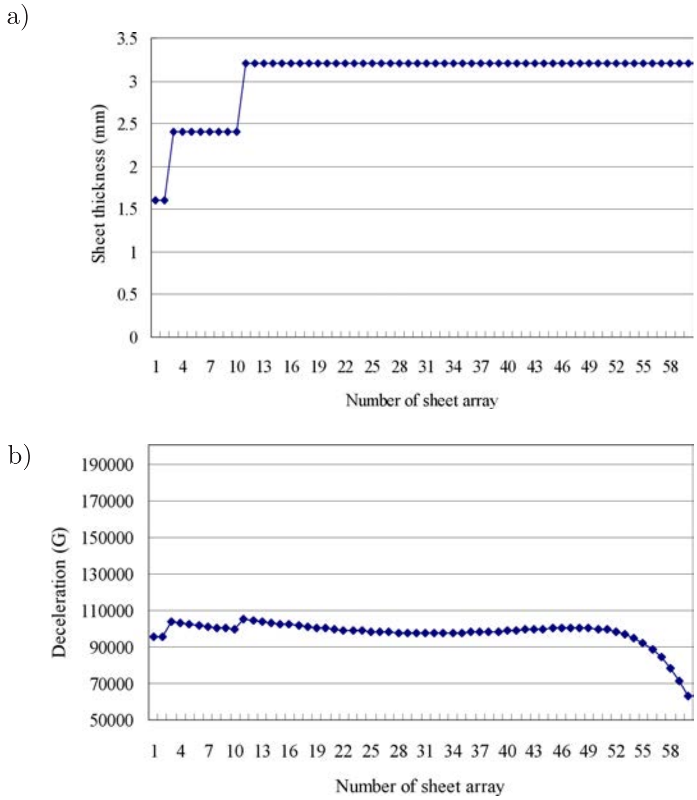

FIG. 2. Estimation of thickness distribution of plate array for soft recovery of projectile: a) thickness distribution of sheet array, b) estimated deceleration of a projectile.

3. Field tests

A soft recovery system was designed and fabricated. It consists of three identical steel frames bolted together to have an overall length of 12 m, Fig. 3. The dimensions of the frame are 900 mm × 900 mm × 4000 mm and the frame is made of 100 mm × 100 mm steel square tube. Each frame can house 19 equally spaced steel square plates of 600 mm × 600 mm which is held by steel clamps at four corners. The steel plates of three different gauges: 0.6 mm, 1.2 mm, and 2.3 mm were tested.

Fig. 3. Soft recovery system with plates installed.

An aluminum foil sensor is glued onto every plate to measure the arrival time of the projectile onto each plate. Dedicated multi-channel time recording system, to conduct this assessment, was developed in-house. The arrival time of the projectile onto each plate was captured successfully and an overall deceleration curve was obtained from the data.

Fig. 4. Velocity measuring equipment (front and rear).

For the field test 180 mm long, a 40 mm caliber hardened steel projectile weighting 1 kg was used and two different guns were used: 40 mm rifled barrel gun and 155 mm smooth bore gun with sabot. The amount of the propellant for each shot was carefully controlled to achieve muzzle velocity of 600 m/s. The sabot assembly launched by 155 mm gun was stopped by the stopper plate while the projectile continued to fly to pierce through steel plates.

After the shot, all the plates were removed, measured, and photographed. The trajectories of the projectile can be reconstructed from postmortem analysis of the plates. The high speed video system was used to record a detailed behavior of the projectile piercing through the plates.

FIG. 5. 40 mm rifled gun.

FIG. 6. 155 mm smooth bore gun.

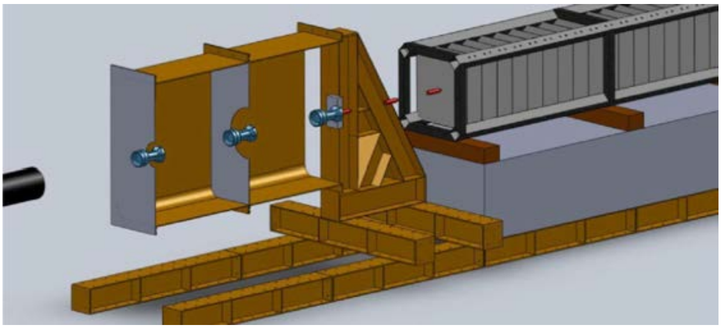

Fig. 7. Schematic of projectile and sabot separation.

Fig. 8. Sabot assembly.

Fig. 9. Deformed plates, front section.

FIG. 10. Deformed plates, mid section.

FIG. 11. Deformed plates end section.

FIG. 12. Projectile wedged in wooden block.

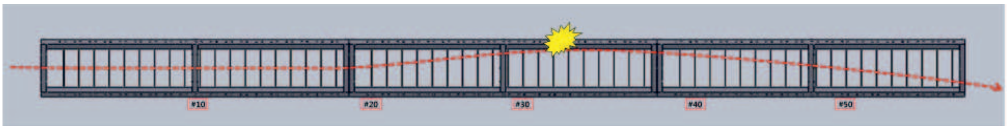

Fig. 13. Trajectory of projectile reconsructed from plates data.

4. Results and discussion

Two different guns were used for the field firing test: a rifled barrel gun and smooth bore gun. Total of eight effective shots were fired by 40 mm rifled gun and three different gauge plates were tested. Only two projectiles were retrieved but were severely deformed and fractured. The clamps holding the plates were often damaged and had to be replaced for subsequent tests. Sections of the frame were also damaged by the high speed projectile exiting out of the frame's sideway. The test results were almost identical regardless of a thickness of the plate. The projectiles veered off from the initial firing line and exited at the mid-section of the frame. Initially, the projectile was piercing through 10–15 plates with no significant yaw angle deviation occurring at two to three meters. Then, the projectile experienced a rapid deceleration caused by fast increase of yaw angle. Finally, the projectile started to tumble. The projectile was deformed and fractured by high impact forces acting from random directions. Once the axis of

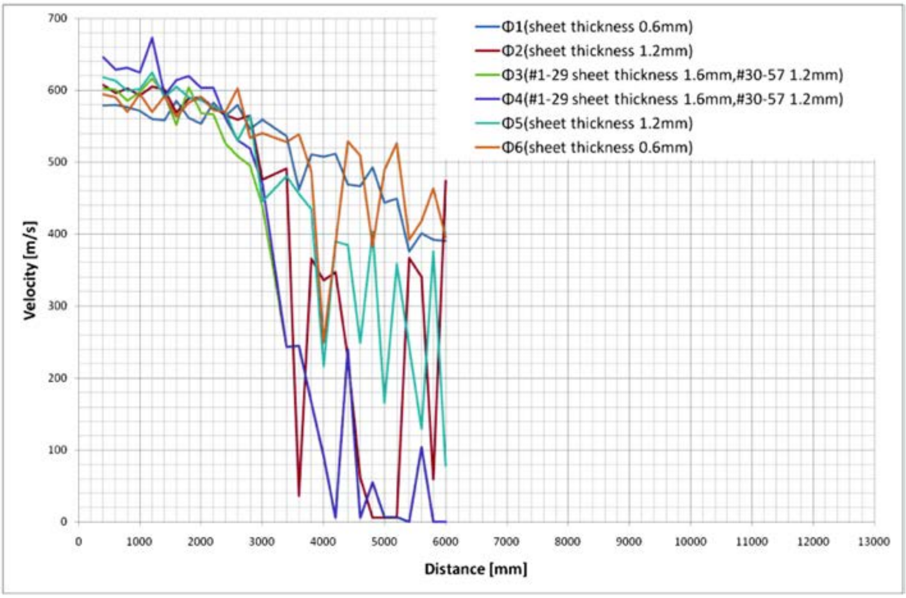

Fig. 14. Distance-velocity data using 40 mm rifled gun.

the projectile is not parallel with flying line, the directions of the stopping forces exerted from the plates are not in the axis of the projectile, i.e., axis-symmetric assumption is no longer valid. Consequently, magnitude of the stopping force increases with the yaw angle.

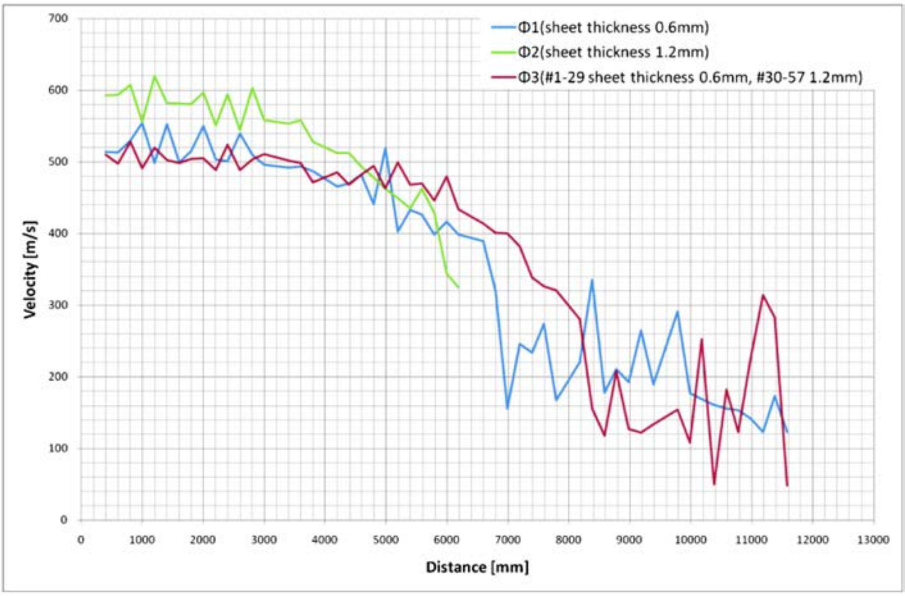

FIG. 15. Distance-velocity data using 155 mm smooth bore gun.

Next, the four effective shots were fired by 155 mm smooth bore gun with plastic sabot assembly. The sabot assembly, launched without a spin, was stopped by stopper plate while the projectile continued to fly, in the end, piercing through steel plates. A short cylinder chunk of the plastic sabot, which punched through the hole of the stopper plate, was following the projectile. This plastic chunk was piercing the larger hole in the plates made in a place where there was already a hole made by the projectile. Thus, the trajectory and posture data were destroyed. Fortunately, the high speed video was operational to record the trajectory and posture data. One projectile was found wedged into the wooden block behind the frame with a minor deformation and another one was found intact on the ground before the end of the frame. According to the high speed video the last projectile entered the test section with initial yaw about 10 degrees thus slowed down much faster and tumbled away. The initial yaw may be caused by a misalignment of the stopper plate in front of the frame. Compared with the rifled gun case, a smooth bore gun test results were more satisfactory, i.e., smooth deceleration span was much longer and projectiles were recovered intact. In the case of 0.6 mm thick plates, the projectile pierced through first

20–30 plates, in a span of four to six meters, with no significant yaw angle deviation. The average deceleration rate, about 0.3%, calculated from the test data agrees well with a numerical simulation estimation. In case of next 10–15 plates, in a span of two to three meters, the deceleration rate increased slightly with a slight increase of yaw angle. Then, the projectile speed was slow enough and the projectile experienced rapid deceleration caused by a fast increase of yaw angle. In Fig. 13 we can find the projectile trajectory reconstructed from the post-mortem analysis of the recovered plates. The projectile was piercing through the plates in a straight manner and started to veer slowly to top- left direction around a half span and changed direction to bottom- right while rubbing with metal clamps about two- thirds of the span. Finally it exited through the end of the frame, then wedged into the wooden block in the back, see Fig. 12. For 1.2 mm thickness case, the same sequence was observed but the projectile stopped in a half length of the span.

For the projectile with a zero spin and zero yaw, the deceleration characteristics can be described by three different zones: (1) smooth and steady deceleration, (2) deceleration rate increases yet remains constant, (3) sudden increase of deceleration. A perfect alignment of the projectile and the plates is the crucial condition for a successful soft- recovery test but it cannot avoid the axis force components. Comparing the results from the two different guns, it is evident that the initial spin of the projectile attributes to a faster yaw increase. The fast yaw angle increase is caused by the gyroscopic force from the interaction between the spinning projectile and the plate. The final phase of an abrupt deceleration begins at critical speed or critical yaw angle.

Even with perfect test condition, the axis symmetric assumption cannot be maintained throughout the test. Hence, further numerical studies of three-dimensional oblique impact behavior of the projectile are required. More tests with different thickness distribution of the plates and careful alignment are needed to complete the soft recovery test.

Acknowledgment

This work was supported by an ADD fundamental research grant to the Korea University of Technology and Education (UD080011GD).

References

1. Goldsmith W., *Review Non-ideal projectile impact on targets*, International Journal of Impact Engineering, **22**, 95–395, 1999.

2. Yoo Y.H., Chang S.N., Chung D.T., *Numerical Simulation of High-Velocity Oblique Impact of Mild Steel Spheres Against Mild Steel Plates*, Journal of KSME, **26**, 3, 576–585, 2002.

3. Park M.S., Yoo J.H., Chung D.-T., *An Optimization of a Multi-Layered Plate under Ballistic Impact*, International Journal of Solids and Structures, **27**, 1, 123–137, 2005.

4. Johnson G.R., Cook W.H., '*Lagrangian EPIC code computations for oblique, yawed-rod impacts into thin-plate and spaced-plate targets at various velocities*, International Journal of Impact Engineering, **14**, 373–383, 1993.

5. Meyers M.A., *Dynamics behavior of materials*, John Wiley & Sons, Inc., New York, 1994.

Received January 11, 2011; revised version August 15, 2011.